Available online at www.sciencedirect.com
ScienceDirect
Polymer Testing 27 (2008) 136–145
POLYMER TESTING
www.elsevier.com/locate/polytest

Test Method

Determination of craze initiation stress in very small polymer specimens

Davide S.A. De Focatiis*, C. Paul Buckley

Department of Engineering Science, University of Oxford, Oxford OX1 3PJ, UK

Received 10 July 2007; accepted 19 August 2007

Abstract

A miniature test method is presented for measuring craze initiation stress in tension on very small specimens of glassy polymers (less than 10 mg). The method consists of three-point bending creep experiments followed by low-power optical microscopy to determine the length of the crazed region, and hence the stress at which crazes initiate within a given time. The test method is especially suitable when extremely limited quantities of material are available. It is illustrated by application to two monodisperse and one polydisperse polystyrenes (PS). In polydisperse PS crazed in diethylene glycol, craze initiation stress and time dependence are close to those of the monodisperse PS with the same M_w, but in polydisperse PS crazed in air, crazes initiate at larger stresses, and the time-dependence is close to that of the monodisperse PS with the same M_n. The findings are discussed in terms of changes in craze initiation mechanisms from disentanglement crazing to chain scission crazing with increasing molecular weight and decreasing time.

Keywords: Craze initiation; Creep; ESC; Polystyrene

1. Introduction

The deformation of glassy polymers such as atactic polystyrene (PS) is frequently accompanied by the initiation and growth of crazes. It is well known that crazes initiate at a stress that decreases with increasing loading time or temperature. In addition, the presence of aggressive environments such as organic fluids also encourages crazing, in a process known as environmental stress crazing or cracking (ESC). The onset of crazing accounts for a substantial proportion of failures in glassy thermoplastic products, and it is not surprising that a considerable amount of work has been published in attempts to characterise, understand and predict the phenomenon [1–7].

This work forms part of a study aiming to improve understanding of the influence of molecular parameters on polymer processing and deformation. With recent advances in polymerisation techniques, it is now possible to obtain small quantities (a few grams) of well-characterised monodisperse polymers with a variety of controlled molecular architectures [8]. To exploit these developments, there is a need for an experimental technique to measure craze initiation stress in very small (<1 g) polymer specimens.

*Corresponding author. Tel.: +44 1865 283487; fax: +44 1865 273906.
E-mail address: davide.defocatiis@eng.ox.ac.uk (D.S.A. De Focatiis).

0142-9418
doi:10.1016/j.polymertesting.2007.08.006

Craze initiation begins with the nucleation of voids in localised regions about 20 nm in diameter which eventually coalesce to produce crack-like surfaces spanned by fibrils of highly oriented polymer [6]. An intrinsic feature of craze initiation and growth is the existence of tensile stress in all directions in the craze plane, which drives cavitation. Thus, under tensile loading, craze formation occurs under plane strain conditions. In addition, since the service loading of many products is bending, the peak stresses and hence craze initiation sites are located at surfaces, and are susceptible to local inhomogeneities and surface defects [9].

A substantial fraction of the published studies of PS crazing has involved microscopy and the use of thin (1–10 μm) films bonded to copper grids [10–16]. The thin films require only small amounts of polymer, but there are several reasons for caution in the application of these tests to the understanding of crazing in bulk polystyrene. Most importantly, the geometry of a thin film with thickness of the same order as the craze thickness imposes conditions of plane stress rather than plane strain. Also, it has been observed that the glass transition temperature (T_g) [17–19] and the bulk modulus [20] of thin films of PS are considerably lower than those of bulk specimens.

Another technique requiring only a small amount of polymer is the micro-indentation technique of van Melick et al. [21]. However, this technique relies on accurate constitutive modelling of the material in order to establish the stresses at craze formation, and crazes are generated below the surface of the specimen. Uniaxial tension techniques have also been used [22] but are impractical to apply to miniature specimens of brittle polymers.

Beam bending experimental techniques are common in crazing experiments, either through the use of an elliptical former [23–25], in three-point bending with a fixed imposed central displacement [26–29], or at constant displacement rate [30,31]. Since the polymer undergoes non-linear viscoelastic stress-relaxation before and after craze formation during the test, the state of stress during crazing is not clearly defined in any of these techniques, and quantitative interpretation is not always possible [32].

The aim of the present paper is to present a miniature test method capable of using sub-gram quantities of polymer to measure craze initiation in bulk polymer specimens under a well-characterised stress state. The technique developed consists of three-point bending creep experiments on miniature rectangular beams followed by low-power optical microscopy to identify the length of the crazed region, and hence the stress at which crazes become visible. The technique is used to measure craze initiation stress in a polydisperse PS and two monodisperse PS, investigating the time dependence of craze initiation in air and in diethylene glycol (DEG). The technique is validated by comparison with results from a similar test using larger specimens.

2. Experimental

2.1. Materials

The materials used in this study include a typical commercial grade of polydisperse atactic (amorphous) PS and two monodisperse atactic PS. Molar mass measurements were kindly performed by Dr Lian Hutchings of the University of Durham, by size exclusion chromatography (SEC) on a Viscotek TDA 302 with refractive index, viscosity and light scattering detectors, and results are given in Table 1 with the codes used to refer to the materials in this paper. Material R was obtained from Dow Chemicals, while materials C and BA were synthesised by living anionic polymerisation at the University of Durham. The molar mass of materials C and BA were chosen in order to be close to the number average and the weight average molar masses of material R, respectively.

2.2. Moulding

PS plates approximately 0.5 mm in thickness were compression-moulded using rectangular moulds in a hand-operated Moore hydraulic press with heated platens. The top and bottom surfaces of the mould were lined each time with a fresh sheet of 0.15 mm thick soft temper 1200 aluminium foil obtained from Multifoil Ltd., in order to provide a repeatable

Table 1
Molar mass measurements and polydispersity obtained by triple detection SEC for the polystyrene samples

Code	M_n (g/mol)	M_w (g/mol)	PDI (M_w/M_n)
R	85,900	218,000	2.54
C	89,700	94,400	1.05
BA	176,000	221,000	1.26

surface roughness. The rolling direction of the foil was always aligned with the eventual direction of the tensile stress in the crazing experiments. The mould was placed between pre-heated press platens and reached 170 °C in approximately 10 min, during which time the platens were slowly closed. The clamping force was then cycled manually for a period of 5 min to dislodge any trapped air bubbles. The mould was then held at 170 °C at moderate pressure for a further 10 min, and cooled to room temperature at a rate of 15 °C/min by forcing water through channels in the press platens. The mould was removed from the press when the temperature reached T_g−20 °C. There is evidence that glass structure plays a role in craze initiation [33]. Care was taken therefore to repeat the moulding procedure identically in order to produce specimens with the same glass structure. The temperature during a typical moulding cycle was monitored with an embedded thermocouple, and is shown in Fig. 1. The mouldings have been verified as being optically isotropic.

In addition, a small batch of larger specimens approximately 2 mm × 5 mm × 60 mm were compression-moulded directly to size using the procedure described above. The top and bottom surfaces of the larger specimen mould were also lined with a fresh sheet of the same aluminium foil used for the miniature samples.

2.3. Miniature specimen preparation

In order to produce miniature beam specimens, parallel-sided strips of material were cut from the 0.5 mm sheets using a custom-made jig with parallel single-bevelled blades. The strips were then trimmed to length, producing rectangular prismatic beams typically 0.5 mm × 2 mm × 8 mm in size, using less than 10 mg of polymer for each specimen. The long axes of the beams were aligned with the rolling direction of the aluminium foil mould liner to give the specimens a reproducible surface roughness.

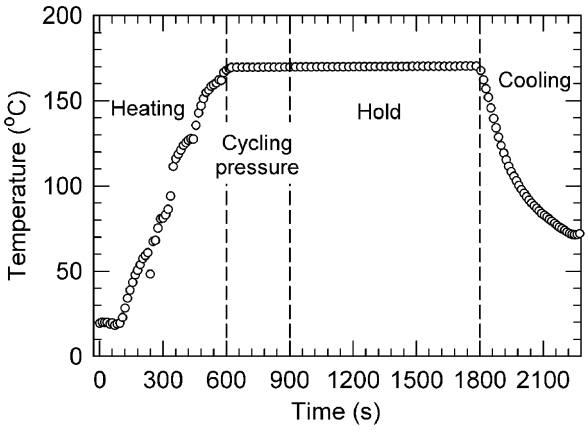

Fig. 1. Temperature recorded during a typical moulding using a thermocouple embedded within the mould.

A small batch of specimens of polymer R was tested dry. All other specimens were soaked in analytical reagent grade DEG for a minimum of 1 day prior to ESC tests. The liquid uptake of larger soaked rectangular plates of polymer R was monitored at regular intervals for 1 week. The average equilibrium solubility, expressed as the volume of liquid absorbed per unit volume of polymer, was 0±0.1% throughout the 1 week period. Kambour et al. [23] measured the equilibrium solubility of DEG in PS as 3.2%. The reason for this discrepancy is not known.

2.4. Miniature creep rig

The miniature three-point bending creep rig was constructed in the authors' laboratory. It consists of adjustable supports mounted on small micrometer lead screws and a load tray connected to a LVDT transducer. The LVDT was mounted on a larger micrometer lead screw for calibration. The load tray applies the load to the specimen beam mid-way between the supports through a lightweight load plate sliding in PTFE guides, providing location but with minimum friction. The three-point bending rig can be placed in a metal tray designed to hold the environmental liquid used. The rig is shown without the liquid tray in Fig. 2. The specimen was placed on the supports and retained in position by the load plate. Typically, the distance between the supports was 5 mm. It was found more convenient to keep the miniature specimen submerged in DEG by positioning a very thin strip of PTFE tape under the specimen and wetting the area with liquid, relying on the surface tension of the liquid to keep it in place, rather than filling the entire tray with DEG.

A larger version of the creep rig was constructed in order to validate the results of the miniature rig. It was designed to operate in a similar fashion with the larger specimens with dimensions 2 mm × 5 mm × 60 mm, and a fixed support spacing of 50 mm.

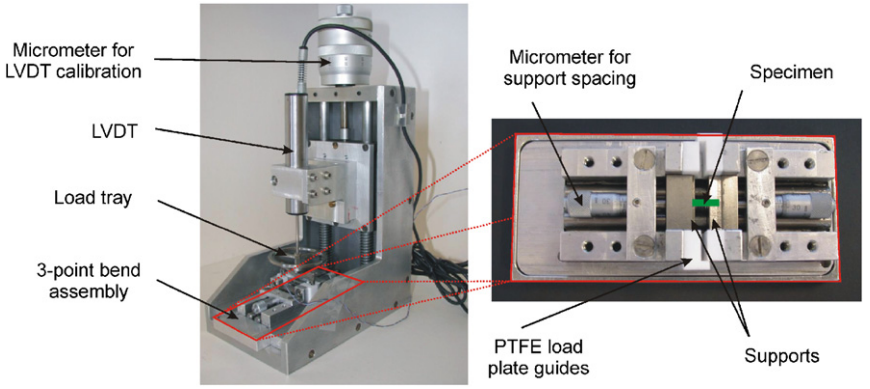

Fig. 2. The three-point bending creep rig. The liquid tray has been removed for clarity. The position of the specimen is artificially highlighted in green.

2.5. Creep and crazing experiments

The experimental set-up may be used to obtain linear viscoelastic creep measurements in three-point bending by the application of a small load. Fig. 3 shows a typical measurement of central displacement, obtained during linear viscoelastic creep (ensuring that the maximum strain in the specimen does not exceed 0.5%) for 300 s in polymer R saturated in DEG.

The same technique is used to induce craze formation in the specimen, by the application of a larger load. Fig. 3 also includes a typical trace of the central displacement obtained during crazing for 300 s in polymer R. Crazed specimens show significant amounts of non-recoverable deformation, as may be seen in Fig. 3 where the load was removed after 300 s.

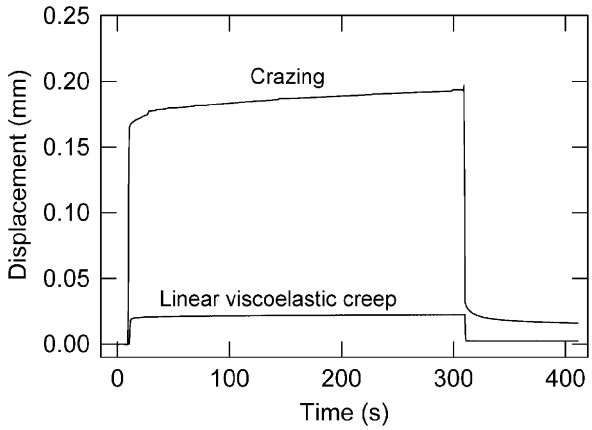

Fig. 3. Sample measurements of central displacement in three-point bending under two loads, during 300 s creep of PS in DEG: creep in the linear viscoelastic region and creep during crazing.

2.6. Stresses in beam bending

The tensile stress experienced by the uncrazed part of the specimen can be described by the elementary theory of bending of slender linear elastic beams. This is true throughout the specimen and the test in linear viscoelastic creep experiments. In crazing experiments, there is always a region near the supports where the stress is insufficient to initiate crazes, and, assuming linear viscoelasticity up to the initiation of crazes (a good assumption in PS), the stress may be obtained from the same theory. In the region in the middle where crazes initiate and relieve local stress through craze growth, the elementary theory is not obeyed. Denoting coordinates x and y with respect to an origin at the centre of the specimen, the tensile stress $\sigma_{xx}(x,y)$ in the region of the specimen obeying elementary beam theory is given by

$$\sigma_{xx}(x,y) = -\frac{My}{I} = -\frac{3P}{bd^3}(l-2x)y, \tag{1}$$

where M is the bending moment, I the second moment of area of the cross-section, P the applied load, b the breadth, d the depth of the beam and l is the span between supports. Fig. 4 shows a graphical representation of the contours of equal tensile stress in the beam given by elementary beam theory.

Every crazing experiment is designed to produce a small but measurable region of approximately triangular shape, located opposite the central load, where crazes initiate.

Fig. 5 shows a larger beam of PS crazed in three-point bending where the approximately triangular region is clearly visible.

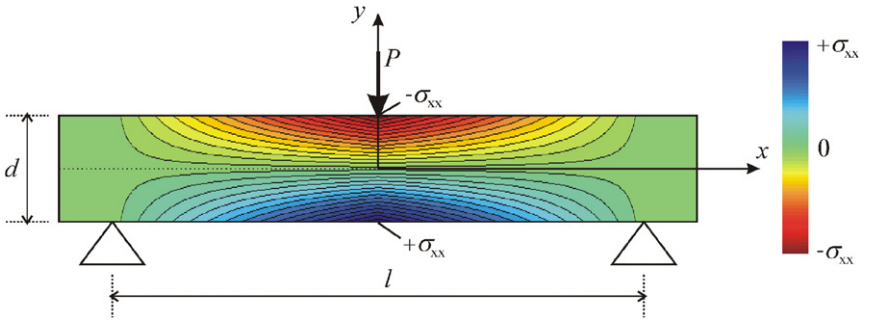

Fig. 4. Contours of equal longitudinal stress in a beam in three-point bending as predicted by elementary beam theory. Tensile stress is denoted as positive.

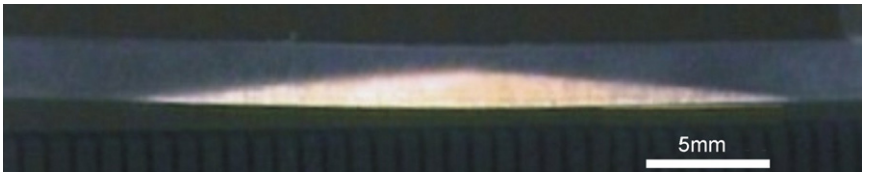

Fig. 5. A larger (2 mm × 5 mm × 60 mm) crazed specimen of PS viewed from the side showing the region of approximately triangular shape where crazes have initiated.

The aim of this technique is, through measurement of the length of the crazed region l_c, to obtain the stress at which crazes have just formed and become visible. Since outside the crazed region elementary beam theory is obeyed, taking $y = -d/2$ and $x = l_c/2$ in Eq. (1) gives an expression for the stress σ_c at which crazes have just formed in the given time as

$$\sigma_c = \frac{3P}{2bd^2}(l - l_c). \quad (2)$$

2.7. Measurement of the length of the crazed region

The miniature crazed specimens were removed from the crazing rig and gently dried with absorbent paper if necessary. They were then located on a custom-made support under a low-power optical microscope with crazes on the upper surface. Crazes were not visible when the specimen was viewed normal to the surface with either reflected or transmitted light. The support was therefore placed at a small angle θ to the horizontal, and a beam of white light was directed to be incident to the crazed specimen at a small angle θ to the crazed beam surface normal through the use of mirrors. The arrangement is illustrated in Fig. 6. A value of $\theta = 10^\circ$ was found to be appropriate. The crazes acted as mirrors, directing the light towards the microscope. Measurements of the length of the crazed region were then made with appropriate calibration. In order to capture crazes whose plane was not exactly perpendicular to the surface, a hand-held mirror was used to vary slightly the incoming angle of the light. Five measurements of the extent of the crazed region were made across the width of each specimen. All measurements were made within 1 h of crazing.

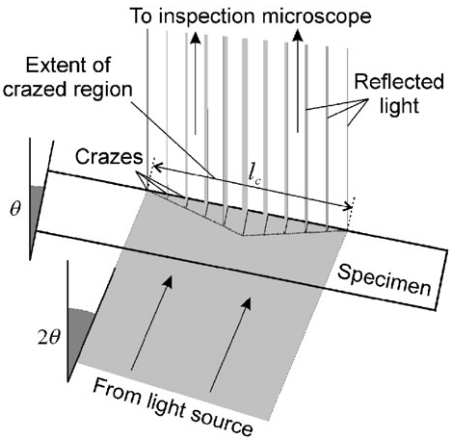

Fig. 6. Measurement of the extent of the crazed region in the miniature specimens through the use of the reflective property of the crazes.

2.8. Imaging miniature crazed specimens

A similar technique was used to produce images of crazed specimens. A prism of the same material as the specimen being imaged was constructed so as to reflect an incoming light beam towards the specimen at a small angle θ to the crazed beam surface normal. The specimen was located on a surface of the prism at a small angle θ to the horizontal with the crazes on the upper surface. The incoming light was reflected from the crazes vertically towards the microscope, as shown in Fig. 7.

The depth of field of the microscope is limited and images were recorded at various points on the specimen in order to maintain focus. The individual images were then cropped and recombined to produce a continuous image of the whole specimen. In order to maintain the correct aspect ratio, the image was subsequently stretched by a factor of $1/\cos\theta$ in the direction of the long axis (x-axis) of the specimen.

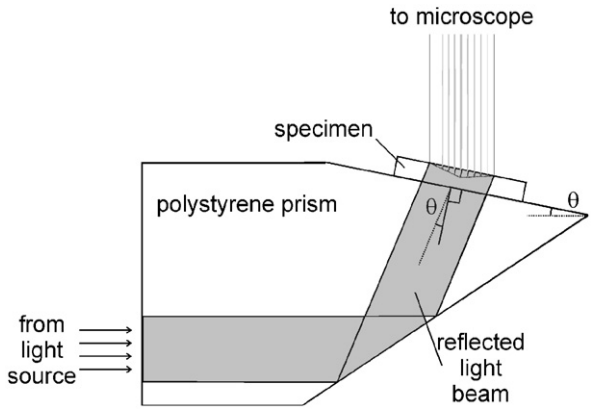

Fig. 7. The prism arrangement used to produce images of crazed specimens with visible crazes.

2.9. Dynamic mechanical analysis

Two small rectangular bars (0.5 mm × 6 mm × 30 mm) of polymer R were tested in bending in a Triton dynamic mechanical analyser (DMA) with fluid bath attachment in tension at 1 Hz at 3 °C/min. The strain amplitude used did not exceed 0.2%. One bar had been saturated in DEG and was held under a bath of DEG throughout the test; the other bar was kept dry before and during the test.

3. Results

3.1. Craze character

A typical image of a specimen of polymer R crazed after 300 s creep in DEG, produced using the technique described in Section 2.8, is shown in Fig. 8. Crazes near the edge of the specimen were approximately 0.2–0.3 mm long and were generally distinct from one another. The fact that they are sharply in focus in Fig. 8 is an indication that the depth of the crazes through the thickness of the specimen is small.

Crazes near the middle of the specimen were generally wider, occasionally reaching the full 2 mm width of the specimen. The depth of crazes also increased near the middle of the specimen and it was difficult to image entire crazes in focus, because of the limited depth of field. Near the edge of the crazed region, there was a relatively regular spacing between crazes of approximately 0.1 mm along the length of the beam. The increase in the density of crazes near the centre of the specimens prevented a reliable estimate of the spacing in that region.

3.2. Validation of miniature specimens

Craze initiation stress was measured after 300 s creep in DEG on a range of miniature specimens of

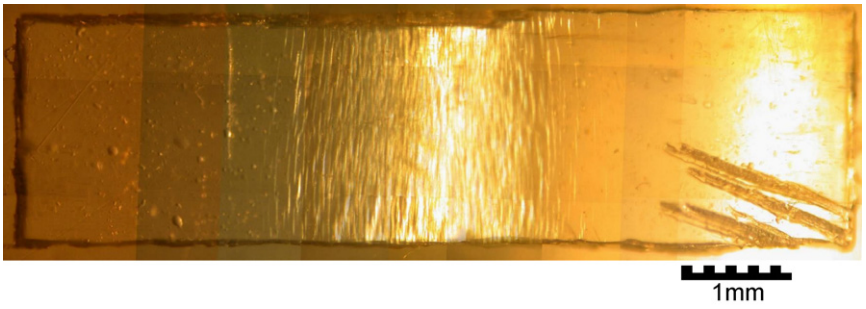

Fig. 8. Image of a crazed specimen of polymer R after 300 s creep in DEG taken using the technique described in Section 2.8. The scratches on the bottom right are used as a marker for identifying the crazed surface of the specimen.

polymer R, varying the support spacing from 2.5 to 8 mm, and varying the load applied such that the peak stress in the specimen varied from 20 to 40 MPa. The results obtained on a sample of 17 tests are $\sigma_c = 16.8 \pm 0.7$ MPa (where $\pm$ represents two standard errors, or the 90% probability that the population mean lies in the given range). The measurements of craze initiation stress were verified with significance at the 5% level as being statistically independent of the length of the support spacing and of the peak stress applied to the sample.

As a validation of the method, the larger version of the creep rig was used with the larger specimens with the same surface roughness and temperature history. Craze initiation stress was measured after 300 s creep in DEG on larger specimens of polymer R. The results obtained on a sample of five tests are $\sigma_c = 15.8 \pm 0.3$ MPa. Craze initiation stress was also measured after 12 and 60 s creep in both the miniature specimens and the larger specimens of polymer R, and in all cases there was no significant difference between the sample means of the miniature and the larger tests at the 95% confidence level.

3.3. Dry crazing

To evaluate the effect of the DEG on crazing, a small number of specimens of polymer R were tested dry. The stress required to initiate crazes was substantially higher than in PS saturated in DEG, and specimens frequently failed by brittle fracture during the creep test. Results obtained on a sample of five tests of those miniature specimens of polymer R that did not fracture in 300 s creep are $\sigma_c = 32.8 \pm 2.6$ MPa.

3.4. Time-dependence

Craze initiation stress was measured after 12, 60 and 300 s creep in DEG on all polymers listed in Table 1. Linear regression was performed on all the available craze initiation stress measurements for each polymer as a function of log creep time in order to establish the time-dependence. The results and regression lines are shown in Fig. 9.

4. Discussion

From the data in Fig. 9, the rate of change of craze initiation stress with log creep time $d\sigma_c/d \log t$ for the three polymers in DEG and for polymer R dry was evaluated and is listed in Table 2. The striking feature of Fig. 9 and Table 2 is the evidence for two distinct craze initiation kinetics: there is one gradient of approximately -1.8 MPa (polymer R in DEG and polymer BA in DEG) and another gradient of approximately -5.0 MPa (polymer R dry and polymer C in DEG). This is explicable in terms of Kramer's observation that for crazing to occur there must be a geometrically necessary entanglement loss [5], and that, depending on the crazing conditions, there are two mechanisms by

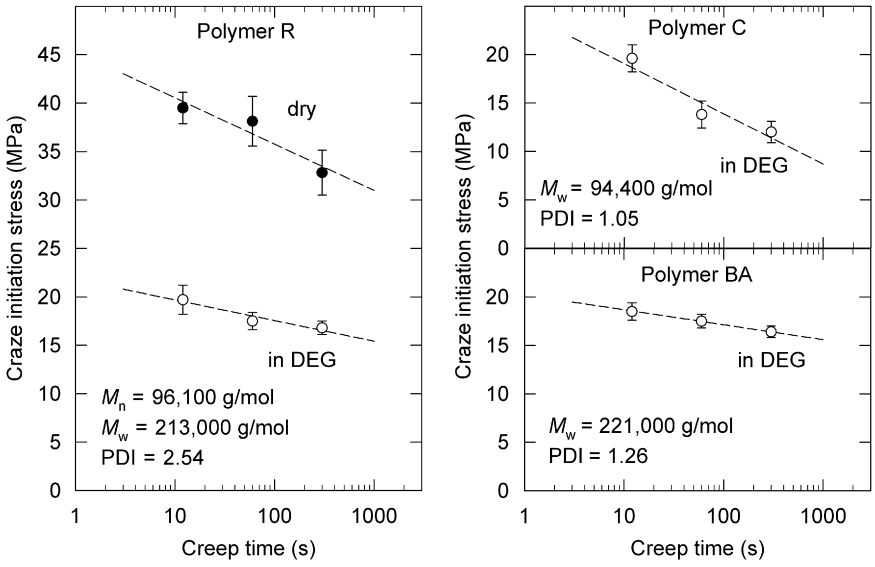

Fig. 9. Craze initiation stress for the three polymers R, C and BA, with linear regression lines through the data. Error bars denote two standard errors.

Table 2
Craze initiation stress and time-dependence for polymers R, C and BA crazed in DEG and dry

Code	300 s creep σ_c (MPa)	$d\sigma_c/d\log t$ (MPa)
R in DEG	16.8 ± 0.7	-2.1 ± 0.2
C in DEG	12.0 ± 1.1	-5.2 ± 0.6
BA in DEG	16.4 ± 0.6	-1.5 ± 0.2
R dry	32.8 ± 2.6	-4.8 ± 0.6

which this may occur: solid-state disentanglement or chain scission [34,35]. Thus, the results above can be rationalised by recognising that different mechanisms dominate under different conditions. Elementary considerations allow us to assign the two gradients to the two processes. Resistance to disentanglement must increase with chain length, while resistance to chain scission is independent of chain length [36]. Thus, the (higher) gradient exhibited by polymer C must be associated with disentanglement, while the (lower) gradient exhibited by the higher molar mass polymer BA must be associated with chain scission. Since chain scission is independent of chain length, we can expect polymer C to switch its craze mechanism where the two curves on the right hand side of Fig. 9 intercept—i.e., close to 10 s. For shorter creep times, crazing by scission is expected for this polymer.

It is interesting to note that polydisperse polymer R exhibits a craze initiation stress, and gradient in Fig. 9, for 300 s creep in DEG, that are close to those of monodisperse polymer BA with a similar *weight* average molar mass M_w, but not to those of monodisperse polymer C, with a similar *number* average molar mass M_n. This suggests that, in the polydisperse polymer, craze initiation is dominated by the behaviour of the high molar mass tail of the polymer, and is equivalent to that of a monodisperse polymer with the same M_w. Other properties of polydisperse polystyrenes such as tensile strength have also been shown to depend on M_w rather than M_n [37].

Another prominent feature in Fig. 9 and Table 2 is the jump in craze initiation stress from 32.8 ± 2.6 to 16.6 ± 0.7 MPa and the switch of craze initiation mechanism, when polymer R is crazed for 300 s in DEG instead of in an air environment. Can this be explained in terms of a change in molecular mobility in the presence of DEG? Loss tangent data from the DMA experiments on specimens of polymer R, tested dry and tested while soaked in DEG, are shown in Fig. 10. From the peaks in Fig. 10, we

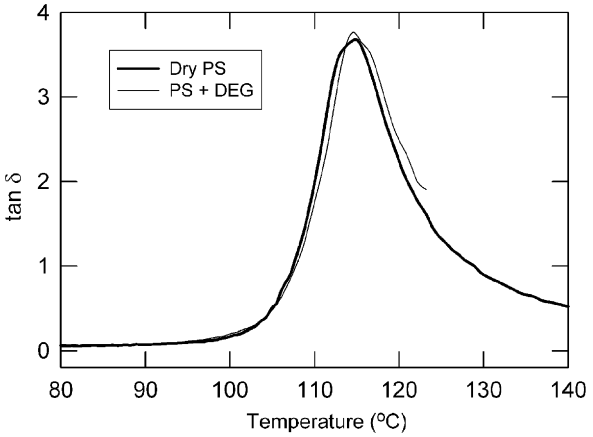

Fig. 10. Loss tangent obtained from DMA at 1 Hz for polymer R dry (thick line) and saturated in DEG (thin line).

obtain a measure of the glass transition temperature (T_g) of dry PS and PS saturated in DEG at 1 Hz as 114.8 and 114.5 °C, respectively. The lack of a significant T_g shift as a result of the DEG is in agreement with the findings of Shah et al. [38] on PS specimens saturated in DEG. The change in craze initiation stress of polymer R cannot, therefore, be attributed to a shift in the glass transition temperature.

It is possible, however, to explain the effect of the DEG environment in terms of its effect on the crazing mechanism. Crazing by chain scission involves the formation of high-energy free radicals at points of scission. However, as is well known in the context of free-radical polymerisation in solution, intimate contact with an organic liquid offers the possibility of transfer of free radicals from polymer to liquid, by the polymer capturing a hydrogen atom [39]. This provides a route to reduction of surface energy of the polymer, and a large reduction of craze initiation stress in the presence of DEG, relative to an air environment, when the mechanism is chain scission. This would explain why polymer R crazes by chain scission when saturated in DEG although it crazes by disentanglement at a much higher stress in air.

A quantitative discussion of these and further results will be given in a forthcoming publication.

5. Conclusions

The miniature test method presented here is capable of using very small rectangular beam specimens weighing only 10 mg to measure craze

initiation stress in polymer specimens under a well-characterised stress state. The method consists of three-point bending creep experiments followed by low-power optical microscopy to determine the size of the crazed region, and, following elementary beam theory, the stress at which crazes initiate and become visible. The test method is applicable to dry polymers and to polymers saturated in liquids. Its validity is demonstrated by the comparison of results with those from larger specimens with the same surface roughness.

The test method has been used to measure craze initiation stress on three well-characterised samples of PS. In the monodisperse materials crazed in the presence of DEG, with increasing molar mass, there is an increase in craze initiation stress and a decrease in its time-dependence. The polydisperse PS has a craze initiation stress and a time-dependence approximating that of the monodisperse polymer with the same weight average molar mass, but significantly different from a monodisperse polymer with the same number average molar mass. This illustrates the dominant role played by the length of the molecules in the polydisperse polymer. In the polydisperse material crazed in air, crazes initiate at larger stresses than in DEG. The time-dependence of the initiation of air crazes is close to that of the low molar mass monodisperse PS crazed in DEG.

The findings are explained in terms of a transition of craze initiation mechanism from disentanglement crazing to chain scission crazing with increasing molar mass and decreasing time. In low molar mass PS, and at longer creep times, disentanglement crazing appears to be the dominant mechanism. The effect of the liquid environment is to lower the stress threshold at which chain scission crazing can take place.

Acknowledgements

The authors wish to acknowledge the help of Dr. Lian Hutchings with the SEC measurements and the synthesis of the monodisperse polymers, and of Gearing Scientific with the DMA experiments. The authors gratefully acknowledge the support of the UK Engineering and Physical Sciences Research Council Grant no. GR/T11845/01.

References

[1] A. Turnbull, T. Maxwell, Test Methods for Environmental Stress Cracking of Polymeric Materials, National Physical Laboratory, 1999.
[2] H.H. Kausch, G.H. Michler, The effect of time on crazing and fracture, Adv. Polym. Sci. 187 (2005) 1–33.
[3] R. Estevez, E. Van der Giessen, Modeling and computational analysis of fracture of glassy polymers, Adv. Polym. Sci. 188 (2005) 195–234.
[4] E.J. Kramer, L.L. Berger, Fundamental processes of craze growth and fracture, Adv. Polym. Sci. 91–92 (1990) 1–68.
[5] E.J. Kramer, Microscopic and molecular fundamentals of crazing, Adv. Polym. Sci. 52–53 (1983) 1–56.
[6] E.J. Kramer, Environmental cracking of polymers, in: E.H. Andrews (Ed.), Developments in Polymer Fracture, Applied Science Publishers Ltd., London, 1979, pp. 55–120.
[7] J.A. Sauer, M. Hara, Effect of molecular variables on crazing and fatigue of polymers, Adv. Polym. Sci. 91–92 (1990) 69–118.
[8] N. Clarke, F.R. Colley, S.A. Collins, L.R. Hutchings, R.L. Thompson, Self-diffusion and viscoelastic measurements of polystyrene star polymers, Macromolecules 39 (3) (2006) 1290–1296.
[9] A.S. Argon, J.G. Hannoosh, Initiation of crazes in polystyrene, Philos. Mag. 36 (5) (1977) 1195–1216.
[10] A.M. Donald, E.J. Kramer, Effect of molecular entanglements on craze microstructure in glassy polymers, J. Polym. Sci., Polym. Phys. Ed. 20 (1982) 899–909.
[11] A.M. Donald, E.J. Kramer, The competition between shear deformation and crazing in glassy polymers, J. Mater. Sci. 17 (1982) 1871–1879.
[12] A.M. Donald, E.J. Kramer, Craze microstructure and molecular entanglements in polystyrene-poly(phenylene oxide) blends, Polymer 23 (1982) 461–465.
[13] A.C.M. Yang, E.J. Kramer, C.C. Kuo, S.L. Phoenix, Crazes in diluted entanglement networks of polystyrene, Macromolecules 19 (7) (1986) 2020–2027.
[14] L.L. Berger, E.J. Kramer, Chain disentanglement during high-temperature crazing of polystyrene, Macromolecules 20 (8) (1987) 1980–1985.
[15] C.J.G. Plummer, A.M. Donald, Disentanglement and crazing in glassy-polymers, Macromolecules 23 (17) (1990) 3929–3937.
[16] H.Z.Y. Han, T.C.B. McLeish, R.A. Duckett, N.J. Ward, A.F. Johnson, Experimental and theoretical studies of the molecular motions in polymer crazing. 1. Tube model, Macromolecules 31 (1998) 1348–1357.
[17] J.A. Forrest, K. Dalnoki Veress, J.R. Stevens, J.R. Dutcher, Effect of free surfaces on the glass transition temperature of thin polymer films, Phys. Rev. Lett. 77 (10) (1996) 2002–2005.
[18] G.B. DeMaggio, W.E. Frieze, D.W. Gidley, M. Zhu, H.A. Hristov, A.F. Yee, Interface and surface effects on the glass transition in thin polystyrene films, Phys. Rev. Lett. 78 (8) (1997) 1524–1527.
[19] J.L. Keddie, R.A.L. Jones, R.A. Cory, Interface and surface effects on the glass-transition temperature in thin polymer films, Faraday Discuss. 98 (1994) 219–230.
[20] K. Miyake, N. Satomi, S. Sasaki, Elastic modulus of polystyrene film from near surface to bulk measured by nanoindentation using atomic force microscopy, Appl. Phys. Lett. 89 (3) (2006) 89–91.
[21] H.G.H. van Melick, O.F.J.T. Bressers, J.M.J. den Toonder, L.E. Govaert, H.E.H. Meijer, A micro-indentation method for probing the craze-initiation stress in glassy polymers, Polymer 44 (8) (2003) 2481–2491.

[22] W. Luo, W. Liu, Incubation time to crazing in stressed poly(methyl methacrylate), Polym. Test. 26 (2007) 413–418.
[23] R.P. Kambour, C.L. Gruner, E.E. Romagosa, Solvent crazing of dry polystyrene and dry crazing of plasticized polystyrene, J. Polym. Sci., Polym. Phys. Ed. 11 (10) (1973) 1879–1890.
[24] M. Kawagoe, T. Ishimi, On the properties of organic liquids affecting the crazing behaviour in glassy polymers, J. Mater. Sci. 37 (23) (2002) 5115–5121.
[25] C.Y. Tang, L.H. Peng, C.C. Li, W. Shen, C.P. Tsui, Experimental study on stable growth of crack and craze damage in HIPS under tension at room temperature, Polym. Test. 20 (3) (2001) 241–251.
[26] G.A. Bernier, R.P. Kambour, The role of organic agents in the stress crazing and cracking of poly(2,6-dimethyl-1,4-phenylene oxide), Macromolecules 1 (5) (1968) 393–400.
[27] P.I. Vincent, S. Raha, Influence of hydrogen-bonding on crazing and cracking of amorphous thermoplastics, Polymer 13 (6) (1972) 283–287.
[28] M.G. Wyzgoski, C.H.M. Jacques, Stress cracking of plastics by gasoline and gasoline components, Polym. Eng. Sci. 17 (12) (1977) 854–860.
[29] Y.W. Mai, Environmental stress cracking of glassy polymers and solubility parameters, J. Mater. Sci. 21 (3) (1986) 904–916.
[30] N.E. Zafeiropoulos, R.J. Davies, K. Schneider, M. Burghammer, C. Riekel, M. Stamm, The relationship between craze structure and molecular weight in polystyrene as revealed by mu SAXS experiments, Macromol. Rapid Commun. 27 (19) (2006) 1689–1694.
[31] A. Turnbull, A.S. Maxwell, S. Pillai, Comparative assessment of slow strain rate, 4-pt bend and constant load test methods for measuring environment stress cracking of polymers, Polym. Test. 19 (2) (2000) 117–129.
[32] J.C. Arnold, The use of flexural tests in the study of environmental stress cracking of polymers, Polym. Eng. Sci. 34 (8) (1994) 665–670.
[33] J.C. Arnold, The influence of physical aging on the creep-rupture behavior of polystyrene, J. Polym. Sci., Part B: Polym. Phys. 31 (11) (1993) 1451–1458.
[34] A.M. Donald, The effect of temperature on crazing mechanisms in polystyrene, J. Mater. Sci. 20 (7) (1985) 2630–2638.
[35] A.C.M. Yang, E.J. Kramer, C.C. Kuo, S.L. Phoenix, Craze fibril stability and breakdown in polystyrene, Macromolecules 19 (7) (1986) 2010–2019.
[36] H.H. Kausch, J.L. Halary, C.J.G. Plummer, Crazing and fracture in polymers: micro-mechanisms and effect of molecular variables, Macromol. Symp. 214 (2004) 17–30.
[37] H.W. McCormick, F.M. Brower, L. Kin, The effect of molecular weight distribution on the physical properties of polystyrene, J. Polym. Sci. 39 (1959) 87–100.
[38] B.A. Shah, M. Shen, G. Akovali, Dynamic mechanical-properties of solvent-crazed polystyrene, J. Appl. Polym. Sci. 23 (1) (1979) 295–298.
[39] F.R. Mayo, Chain transfer in the polymerization of styrene: the reaction of solvents with free radicals, J. Am. Chem. Soc. 65 (1943) 2324–2329.